Electrocatalytic Fischer–Tropsch Reactions. Formation of Hydrocarbons and Oxygen-Containing Compounds from CO on a Pt Gas Diffusion Electrode

Kohjiro Hara, Noriyuki Sonoyama, and Tadayoshi Sakata*

Department of Electronic Chemistry, Interdisciplinary Graduate School of Science and Engineering, Tokyo Institute of Technology, 4259 Nagatsuta Midori-ku, Yokohama 226

(Received October 2, 1996)

Electrocatalytic reduction of CO under high pressure (< 60 atm) using a gas diffusion electrode containing Pt catalyst (Pt-GDE) has been investigated. Acetic acid was formed at a high faradaic efficiency of 32% as a predominant CO reduction product at a constant current density of 200 mA cm^{-2} under CO 40 atm. Moreover, methane, ethane, ethylene, formaldehyde, acetaldehyde, ethanol, 1-propanol, and allyl alcohol were produced as CO reduction products. The selectivity of the reduction products depends remarkably on electrolysis conditions such as the current density, pressure of CO, and temperature. C2-compounds such as ethylene, ethanol, and acetic acid were preferentially formed at small current densities and/or high CO pressure conditions, whereas methane was predominantly produced at large current densities and/or low CO pressure conditions.

In the last decade, fixation of CO_2 which has a low reactivity for reactions, has attracted considerable attention from both industrial and scientific viewpoints. The electrochemical reduction of CO_2 using various metal electrodes in aqueous electrolytes has been extensively investigated as one of methods of chemical fixation of CO_2 by many workers. It was found that the selectivity of the reduction products strongly depends on the kind of metal electrode, and it is clarified that metals can be divided into several main groups from the location in the periodic table[1—7] Interestingly, Hori et al. found that methane and ethylene were produced as the main products, in addition ethanol, acetaldehyde, and 1-propanol were also formed only in the case of Cu electrode.[1,8—10] However, little methane and ethylene are formed and the predominant reduction product is CO in the cases of Ag, Au, and Zn electrodes which are located near to Cu in the periodic table. The reason why hydrocarbons and alcohols form at high faradaic efficiency only on Cu electrode has not been clarified yet. Formation of hydrocarbons from CO_2 is observed at several metal electrodes in addition to the Cu electrode. For example, Frese et al. reported methane formation in the electrochemical CO_2 reduction on Ru electrode at high temperature (< 80 °C) in aqueous electrolyte.[11] In addition, hydrocarbons such as methane, ethane, ethylene, propane, and butane were formed from CO_2 at several % of faradaic efficiencies on Fe, Ni, Co, and Pd electrodes under 1 atm CO_2 and high pressure conditions.[12—16]

It is thought that CO is the intermediate in the formation of hydrocarbons by the electrochemical reduction of CO_2 on metal electrodes. Hori et al. investigated the electrochemical reduction of CO on a Cu electrode at a constant current density of 2.5 mA cm^{-2} in 0.1 mol dm^{-3} $KHCO_3$ aqueous electrolyte. They reported that methane, ethylene, and ethanol were formed at faradaic efficiencies of 16.3, 21.2, and 10.9%, respectively.[10] They concluded that carbon monoxide is produced firstly at Cu electrode on the electrochemical reduction of CO_2, and then CO is reduced electrochemically into hydrocarbons and alcohols. The result that the predominant CO_2 reduction product is not methane and ethylene but CO at positive potential than −1.3 V vs. NHE even on Cu electrode,[10] can be explained by the above suggestion. In addition, it was shown that hydrocarbons formed on Fe, Ni, Co, and Pd electrodes follows well Schultz–Flory distribution. It suggests that the mechanism of hydrocarbon formation on these electrodes is similar to that of Fischer–Tropsch reaction.[6,15—18] Absorbed CO formed on Cu and Ni electrodes studied by FTIR were reported.[19,20]

Recently, authors have investigated the electrochemical reduction of CO_2 under high pressure using a gas diffusion electrode containing Pt catalyst (Pt-GDE).[21,22] As a result, CO_2 reduction at a partial current density of 415 mA cm^{-2} was achieved; methane, ethanol, ethylene, carbon monoxide, and formic acid were produced as CO_2 reduction products at a constant current density of 900 mA cm^{-2} under 30 atm. Methane was produced at the faradaic efficiency of 35% with the partial current density of 313 mA cm^{-2}. The selectivity of the reduction products depended remarkably on the electrolysis condition such as configuration of the electrode, current density, CO_2 pressure, and the reaction temperature. It was suggested that carbon monoxide was an intermediate for the formation of methane, ethylene, and ethanol on the electrochemical reduction of CO_2 on the Pt-GDE in the same way as at Cu, Ni, and Fe electrodes. From the comparison between the selectivity of the products of the CO_2 reduction

and that of the CO reduction, we expect to obtain important information concerning the reaction mechanism of the CO_2 reduction. From this viewpoint, we have investigated the electrochemical reduction of CO under high pressure using Pt-GDE, and report the results in this publication.

It is well-known that various hydrocarbons, alcohols, and organic acids have been industrially synthesized from CO and H_2 (synthesis gas), catalyzed with various metals and metal complex catalysts, whereas the industrial catalytic reactions using CO_2 are rare. This indicates that the reaction activity of CO in these catalytic reactions is higher than that of CO_2. From this viewpoint, the selectivity of the products in the electrocatalytic reduction of CO is very interesting. We have also studied the electrochemical reduction of CO on a Pt-GDE in detail, in order to investigate the possibility of the electrocatalytic Fischer–Tropsch reaction. We report the effects of the pressure, the current density, and the reaction temperature on the selectivity of reduction products in this publication.

Experimental

Electrolysis Electrolyses under high pressure were conducted in a glass cell fixed in a stainless steel autoclave, as described in the previous publication.[22] The aqueous electrolyte was 45 mL of 0.5 mol dm^{-3} $KHCO_3$ aqueous solution prepared from reagent grade chemicals and distilled water (Wako Pure Chemical Industries, Ltd.). The electrolyte was purified by pre-electrolyses with a Pt black cathode under Ar atmosphere for 15 h to eliminate heavy metal impurities. Electrolyses were conducted without separation between cathode and anode. A magnetic stirrer was used for agitation of the electrolyte and the gas phase. The reference electrode was a Ag/AgCl/sat. KCl and a Pt wire was employed as counter electrode. Carbon monoxide (99.95%) was used without purification and introduced to the gas phase compartment. The configuration of the cell is the following:

high pressure CO/Pt-GDE/electrolyte/Pt

A GDE containing a Pt electrocatalyst and a stainless steel mesh current collector (the amount of incorporated Pt: 0.56 mg cm^{-2}, apparent surface area: 1 cm^2) was purchased from Tanaka Noble Metal, Ltd., and was employed as the working electrode. The structure and configuration of the Pt-GDE was described in the previous paper.[22] A Pt-GDE consists of two layers, i.e. the catalyst layer containing Pt catalyst and the gas diffusion layer. In the present experiments, the GDE was mainly used at the configuration in which the catalyst layer is directed toward the gas phase and the gas diffusion layer faces the electrolyte (the reverse configuration). A GDE without a Pt catalyst purchased from Tanaka Noble Metal, Ltd., was also used for the control experiment. The hydrogen pretreatment of the Pt-GDE was carried out for 1 h under hydrogen atmosphere at 220 °C before electrolysis. After the bubbling of CO for 20 min to exchange the atmosphere, a known pressure of CO was introduced into the autoclave. The electrolyses were conducted galvanostatically at passage of 150 C at 25 °C using a potentiostat-galvanostat (Hokuto, HA-501 and 305) connected in series with a coulomb meter (Hokuto, HF-201). The electrode potential was corrected and measured with an IR compensation instrument (Hokuto, HI-203).

Analysis of the Reduction Products. Quantitative analysis of the electrolysis products contained in the gas phase were conducted by using the following instruments. A gas chromatograph (Ohkura GC-202) equipped with a VZ-10 column (4 mm×2 m) and flame ionization detector (FID) for hydrocarbons and a gas chromatograph (Ohkura GC-802) equipped with an active carbon column (4 mm×2 m) and a thermal conduction deterctor (TCD) for hydrogen were used for this purpose. Ethanol, formaldehyde, acetaldehyde, 1-propanol, and allyl alcohol contained in the liquid phase were analyzed with a gas chromatograph (Ohkura GC-103) equipped with a Porapak QS column (4 mm×2 m) and a FID. Acetic acid was analyzed by a high pressure liquid chromatograph (HPLC, Shimadzu LC-4A equipped with a column (Shodex-Ionpack KC-811, 8 mm×300 mm) and a UV detector (220 nm)). The faradaic efficiencies of reduction products were calculated from the following reaction equations.

$$CO + 2H^+ + 2e^- \rightarrow HCHO$$
$$2CO + 4H^+ + 4e^- \rightarrow CH_3COOH$$
$$CO + 6H^+ + 6e^- \rightarrow CH_4 + H_2O$$
$$2CO + 6H^+ + 6e^- \rightarrow CH_3CHO + H_2O$$
$$2CO + 8H^+ + 8e^- \rightarrow C_2H_4 + H_2O$$
$$2CO + 8H^+ + 8e^- \rightarrow C_2H_5OH + H_2O$$
$$2CO + 10H^+ + 10e^- \rightarrow C_2H_6 + 2H_2O$$
$$3CO + 10H^+ + 10e^- \rightarrow C_3H_5OH + 2H_2O$$
$$3CO + 12H^+ + 12e^- \rightarrow 1\text{-}C_3H_7OH + 2H_2O$$
$$2H^+ + 2e^- \rightarrow H_2$$

The limit amounts of the reduction products for quantitative analysis are the following: CH_4 5.1×10^{-8} mol (0.02%), C_2H_4 2.9×10^{-8} mol (0.01%), C_2H_6 2.7×10^{-8} mol (0.02%), HCHO 1.9×10^{-6} mol dm^{-3} (0.01%), CH_3COOH 2.4×10^{-5} mol dm^{-3} (0.3%), CH_3CHO 5.3×10^{-7} mol dm^{-3} (0.01%), C_2H_5OH 3.6×10^{-7} mol dm^{-3} (0.01%), C_3H_5OH 1.9×10^{-7} mol dm^{-3} (0.006%), $1\text{-}C_3H_7OH$ 2.0×10^{-7} mol dm^{-3} (0.007%).

Result

Current Density Dependence of the Products. The electrochemical reduction of CO under 20 atm on a Pt-GDE at the reverse configuration in 0.5 mol dm^{-3} $KHCO_3$ aqueous solution was conducted. As a result, CO was efficiently reduced and methane, ethylene, ethanol, formaldehyde, acetaldehyde, 1-propanol, and allyl alcohol were produced as products of CO reduction. Interestingly, acetic acid which was hardly produced in the electrochemical reduction of CO_2 on a Pt-GDE, was formed at high faradaic efficiency. Faradaic efficiencies of the reduction products formed in the electrolyses under 20 atm CO at current densities 50—600 mA cm^{-2} are shown in Table 1. Figure 1 shows the dependence of faradaic efficiencies of methane, ethylene, ethanol, acetic acid, and hydrogen formations on the current density under CO 20 atm, and Fig. 2 shows that of formaldehyde, acetaldehyde, allyl alcohol, and 1-propanol. However, no methanol formation was observed in this electrochemical system (the limit amount of methanol for analysis is 8.8×10^{-7} mol dm^{-3}, corresponding to 0.02% of faradaic efficiency).

As shown in Table 1 and Fig. 1, the faradaic efficiency for methane formation increases with increasing the current density (16% at 50 mA cm^{-2}, 27% at 100 mA cm^{-2}, and 42% at 200 mA cm^{-2}, respectively) and decreases at current density larger than 200 mA cm^{-2}. The faradaic efficiency of ethylene was 12% at 50 mA cm^{-2}, 9.4% at 100 mA cm^{-2}, and 2.6% at 200 mA cm^{-2}, respectively. Faradaic efficiencies

Table 1. Effect of Current Density on the Electrochemical Reduction of High Pressure CO on a Pt-GDE

Current density	$E^{a)}$	Faradaic efficiency/%										
mA cm^{-2}	V	CH_4	C_2H_4	HCHO	CH_3CHO	C_2H_5OH	C_3H_5OH	1-C_3H_7OH	2-C_3H_7OH	CH_3COOH	H_2	Total
50	−1.79	16.1	12.2	0.43	0.42	5.4	1.1	1.4	N$^{b)}$	34.7	24.4	96.3
100	−1.80	27.2	12.2	0.43	0.23	4.2	0.56	0.90	N	23.4	12.1	81.4
200	−1.83	42.2	9.4	0.31	N	5.1	0.02	0.92	0.07	18.7	10.8	87.7
300	−1.95	27.2	2.6	0.12	N	3.4	Trace	0.38	0.05	2.6	57.4	93.9
600	−1.97	17.1	1.0	0.10	N	2.6	N	Trace	Trace	Trace	80.1	101.0

CO pressure, 20 atm; passed charge, 150 C; electrolyte, 45 mL of 0.5 mol dm^{-3} $KHCO_3$; working electrode, Pt-GDE (apparent surface area, 1 cm^2) which was used for the reverse arrangement. a) Corrected with an IR compensation instrument (vs. Ag/AgCl). b) Not detected.

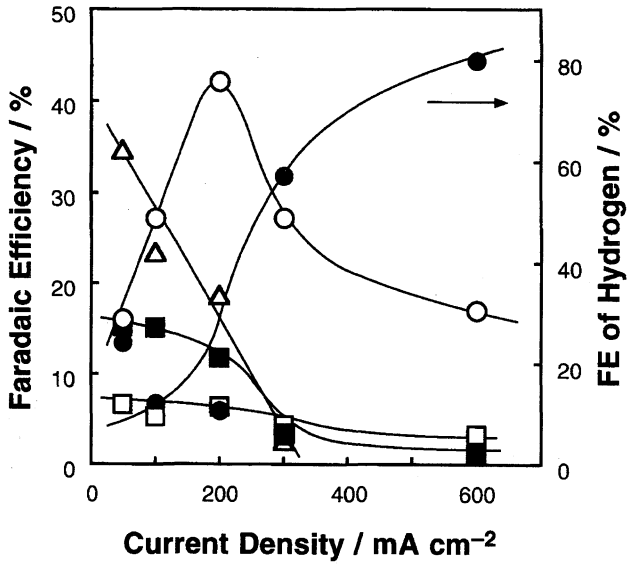

Fig. 1. The current density dependence of the reduction products formed on a Pt-GDE under 20 atm CO at the reverse configuration: (○) CH_4; (■) C_2H_4; (□) C_2H_5OH; (△) CH_3COOH; (●) H_2.

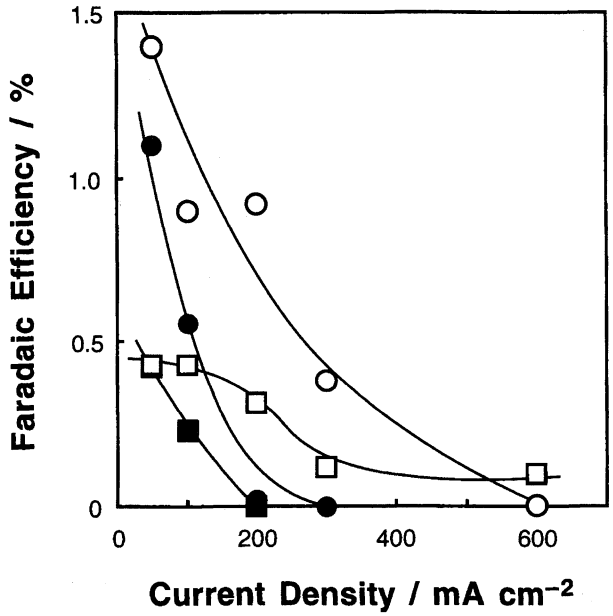

Fig. 2. The current density dependence of the reduction products formed on a Pt-GDE under 20 atm CO at the reverse configuration: (□) HCHO; (■) CH_3CHO; (○) 1-C_3H_7OH; (●) C_3H_5OH.

of ethylene and ethanol decrease with increasing the current density. The faradaic efficiency for acetic acid reaches 35% at 50 mA cm^{-2}, and decreases with increasing the current density (19% at 200 mA cm^{-2} and 2.6% at 300 mA cm^{-2}). The current density dependence of acetic acid is similar to those of ethylene and ethanol. Hydrogen was formed as the main reduction product at the faradaic efficiency of 80% by the reduction of H_2O (or H^+) at the current density of 600 mA cm^{-2}. As shown in Fig. 1, C2-compounds such as acetic acid, ethylene, and ethanol were preferentially produced at small current density and methane was formed as the main CO reduction product at larger current density than that at which preferential formation of C2-compounds were observed. In other words, the main reduction product formed on Pt-GDE was varied in the order of C2-compounds, methane, and hydrogen with increasing the current density. As shown in Fig. 2, formaldehyde, acetaldehyde, allyl alcohol, and 1-propanol were also produced preferentially at small current densities as well as C2-compounds. The potentials of the working electrode during the constant current electrolysis are shown in Table 1. These potentials hardly changed at all during the electrolysis.

Effect of CO Pressure. Results of the CO pressure dependence of faradaic efficiencies of the reduction products formed on a Pt-GDE at the reverse configuration at 200 mA cm^{-2} at passage of 150 C are shown in Figs. 3 and 4. As shown in Fig. 3, hydrogen was formed as the predominant reduction product at faradaic efficiency of 95% under CO 1 atm. The faradaic efficiency of hydrogen decreases drastically and those of products of CO reduction increase with increasing the CO pressure. The faradaic efficiency for methane formation was 4.4% at 1 atm of CO, 26% at 5 atm, and 45% at 10 atm and decreases beyond 10 atm (38% at 40 atm and 31% at 60 atm). The same tendency that the faradaic efficiency of hydrogen decreases drastically and that of methane increases with increasing the reactant pressure was also observed in the electrochemical reduction of CO_2 on a Pt-GDE.[21,22] The maximum faradaic efficiencies of ethylene and ethanol were the same 11% at 40 atm and at 60 atm, respectively. Acetic acid was produced at faradaic efficiencies of 17% at 10 atm and 19% at 20 atm, respectively, and the maximum is 32% at 40 atm, while no

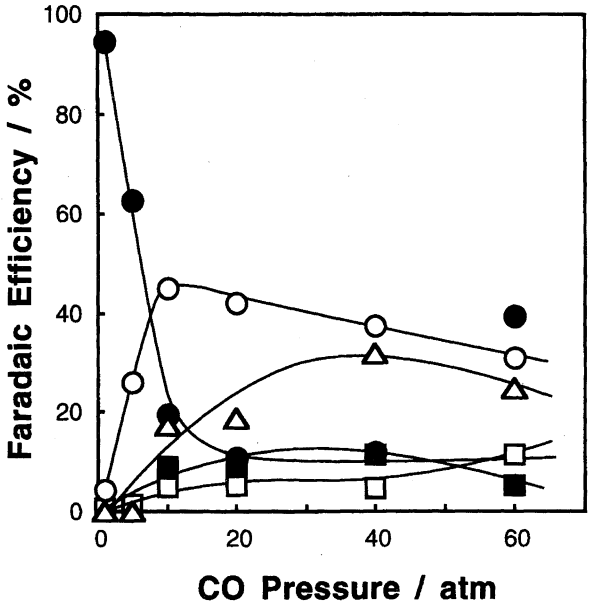

Fig. 3. The CO pressure dependence of the reduction products formed on a Pt-GDE at 200 mA cm^{-2} at the reverse configuration: (○) CH_4; (■) C_2H_4; (□) C_2H_5OH; (△) CH_3COOH; (●) H_2.

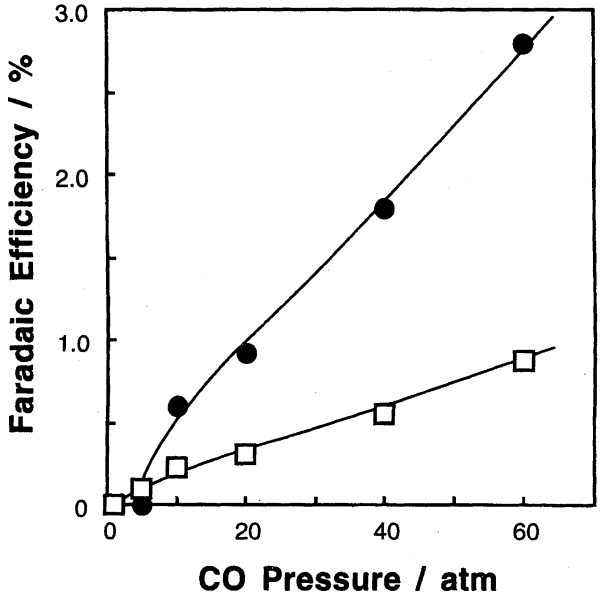

Fig. 4. The CO pressure dependence of the reduction products formed on a Pt-GDE at 200 mA cm^{-2} at the reverse configuration: (■) HCHO; (●) 1-C_3H_7OH.

acetic acid formation was observed under 1 and 5 atm. The partial current density of acetic acid formation reaches 64 mA cm^{-2} at 40 atm. Faradaic efficiencies of formaldehyde and 1-propanol also increases monotonously with increasing the CO pressure, as shown in Fig. 4.

The above CO pressure dependence of reduction products shows that main reduction product changes in the order of hydrogen formed by reduction of H_2O, methane, and C2-compounds such as ethylene, ethanol, and acetic acid with increasing the CO pressure.

Effect of Temperature. Temperature dependence of faradaic efficiencies of methane, ethylene, acetic acid, and hydrogen formed on a Pt-GDE at the reverse configuration under 20 atm at a constant current density of 100 mA cm^{-2} at passage of 150 C, is shown in Fig. 5. The faradaic efficiency of methane decreases with increasing the temperature (47% at 0 °C, 27% at 28 °C, 4.8% at 60 °C, and 1.2% at 80 °C, respectively), while that of hydrogen increases. Ethylene were formed at faradaic efficiencies of 6% at 0 °C, 12% at 28 °C, 10% at 60 °C, and 5.6% at 80 °C, respectively, as shown in Fig. 5. The temperature dependence of the faradaic efficiency of acetic acid is similar to that of ethylene. Interestingly, faradaic efficiencies of ethylene and acetic acid were hardly changed by increasing temperature, while that of methane decreases drastically. Thus, the temperature dependence of faradaic efficiencies of reduction products depended strongly on the kind of products.

Tafel Plot. Figure 6 shows Tafel plots of methane, ethylene, ethanol, acetic acid, and hydrogen formed under 20 atm CO on a Pt-GDE in the case of the reverse configuration These Tafel plots were obtained from the electrode potential during the electrolysis and partial current densities of reduction products calculated from the faradaic efficiencies. As shown in Fig. 6, the partial current densities of the CO reduction products such as methane, ethylene, and ethanol level off at −1.85 V vs. Ag/AgCl presumably because of the mass transfer limitation of CO, while that of hydrogen increases with increasing the electrode potential in the cathodic direction. The partial current densities of methane and ethanol formations are constant at more negative potentials than −1.85 V, while those of ethylene and acetic acid decrease, as

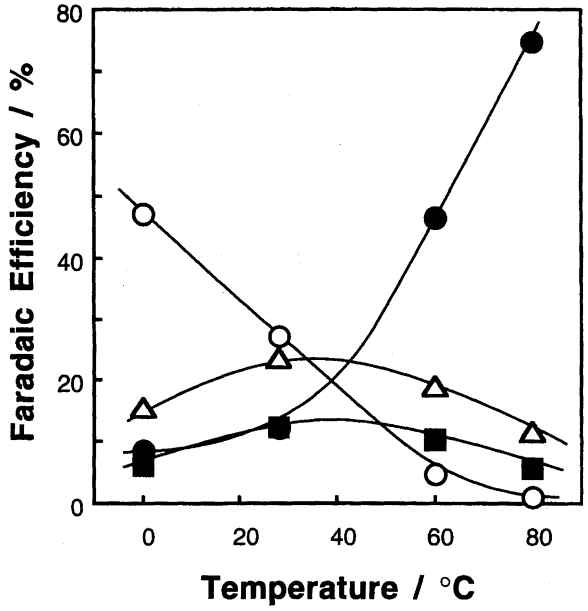

Fig. 5. The temperature dependence of the reduction products formed on a Pt-GDE under 20 atm CO at 100 mA cm^{-2} at the reverse configuration: (○) CH_4; (■) C_2H_4; (△) CH_3COOH; (●) H_2.

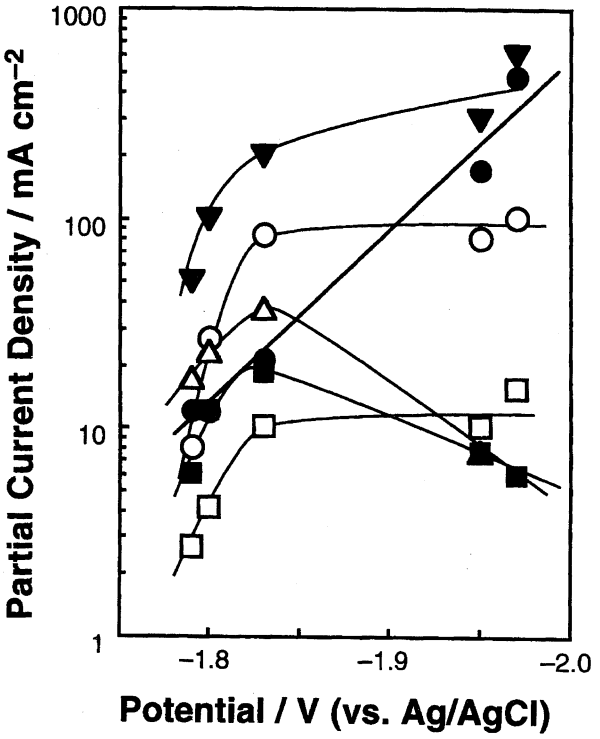

Fig. 6. Tafel plots of the reduction products formed on the electrochemical reduction of CO under 20 atm on a Pt-GDE at the reverse configuration: (○) CH_4; (■) C_2H_4; (□) C_2H_5OH; (△) CH_3COOH; (●) H_2; (▼) total.

shown in Fig. 6. Thus the products of CO reduction can be classified into two groups based on the behavior of the Tafel plot. The maximum partial current densities of methane, ethylene, ethanol, and acetic acid formations under CO 20 atm were 102.6 mA cm^{-2}, 18.8 mA cm^{-2}, 15.6 mA cm^{-2}, and 37.4 mA cm^{-2}, respectively.

Effects of the Pt Catalyst and Electrode Configuration. Table 2 indicates effects of the Pt catalyst and configuration of the electrode on the faradaic efficiencies of the reduction products formed at a constant current density of 200 mA cm^{-2} under CO 20 atm. Firstly, in the case of GDE with Pt catalyst, CO reduction products such as methane, ethylene, acetic acid, ethanol, and 1-propanol were produced at high faradaic efficiencies at the reverse configuration, as has been already shown above. However, in the case of the normal configuration, hydrogen was the predominant product and CO reduction products were hardly produced at all, even on a Pt-GDE. The electrode potential measured during the electrolyses are −1.83 V vs. Ag/AgCl at the reverse configuration and −1.47 V at the normal configuration, indicating a smaller overpotential for the electrode reaction at the normal configuration, compared with the reverse configuration.

In the case of the GDE without Pt catalyst, the predominant reduction product was hydrogen regardless of the electrode configuration, as shown in Table 2. However, methane were produced even without Pt catalyst at normal and reverse configurations at faradaic efficiencies of 0.34 and 2.8%, respectively. The result that methane formation was observed in the case of GDE without Pt catalyst indicates that carbon contained in the GDE has electrocatalytic activity of methane formation from CO. Faradaic efficiency of CO reduction with Pt catalyst was 79.3%, while that without Pt catalyst was 4.1%, as shows in Table 2. This result indicates that Pt catalyst participates in the CO reduction. These results also show that the Pt catalyst and configuration of the electrode are important for the CO reduction on the GDE.

Effect of Hydrogen Pre-treatment of the Pt-GDE. Figure 7 shows the effect of the hydrogen pre-treatment of the Pt-GDE on faradaic efficiencies of methane and ethylene formed at 200 mA cm^{-2} under 20 atm CO. The yield of methane increases with increasing the charge passed until 150 C and levels off after 150 C without hydrogen pre-treatment. This result indicates that the electrocatalytic activity of methane formation of Pt-GDE decreases drastically after 150 C without hydrogen treatment. The yield of ethylene formed on Pt-GDE without hydrogen treatment increases with increasing the charge passed until 700 C. However it is only 13 μmol at 700 C. On the other hand, when hydrogen treatment of Pt-GDE was conducted, the yield of methane increases until 900 C and reaches 363 μmol, which is 3 times larger than that without pre-treatment at 700 C. The yield of ethylene reaches 79 μmol, which is 6 times larger than that without hydrogen treatment at 900 C. It is clear that the electrocatalytic activity of methane and ethylene formations of Pt-GDE improved drastically by the hydrogen pre-treatment of the GDE. In the case of electrochemical CO_2 reduction on Pt-GDE at 600 mA cm^{-2} under 30 atm CO_2 at the reverse arrangement, similar, deterioration of the electrocatalytic activities was observed in the CO and methane formation from CO_2 after passing a change of 250 C,[21] as

Table 2. Effect of the Pt Catalyst and the Electrode Configuration on the Electrochemical Reduction of High Pressure Carbon Monoxide on the GDE

Catalyst	Configuration	$E^{a)}$	Faradaic efficiency/%							
		V	CH_4	C_2H_6	C_2H_4	C_2H_5OH	CH_3COOH	H_2	CO red.$^{b)}$	Total
—	Normal	−1.92	0.34	0.03	0.04	N	N	92.7	0.4	93.1
—	Reverse	−1.92	2.8	Trace	0.24	N	1.0	94.1	4.1	97.2
Pt	Normal	−1.47	Trace	N	N	N	N	100.8	0.0	100.8
Pt	Reverse	−1.83	42.2	0.16	9.4	5.1	18.7	10.8	79.3	87.7

CO pressure, 20 atm; current density, 200 mA cm^{-2}; passed charge, 150 C; electrolyte, 45 mL of 0.5 mol dm^{-3} $KHCO_3$. a) Corrected with an IR compensation instrument (vs. Ag/AgCl). b) The total faradaic efficiency for CO reduction.

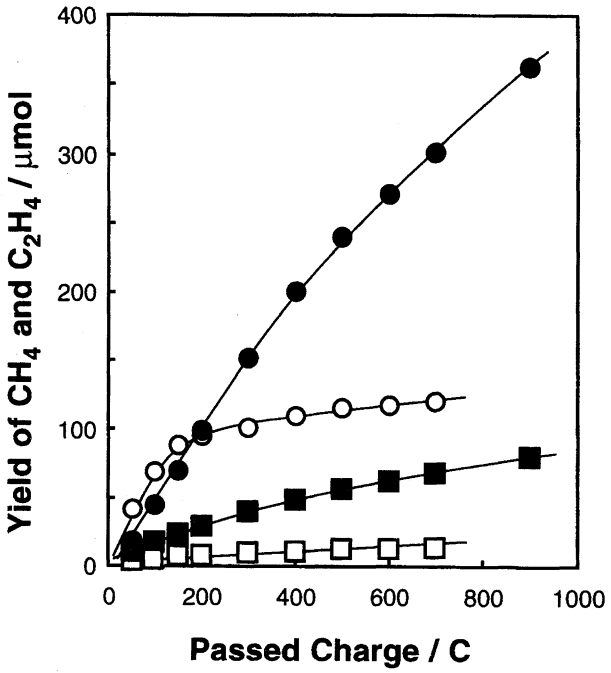

Fig. 7. The passed charge dependence of yields of methane and ethylene formed on a Pt-GDE at 200 mA cm^{-2} under 20 atm CO at the reverse configuration: (○) CH_4; (□) C_2H_4 without hydrogen pretreatment of GDE, (●) CH_4; (■) C_2H_4 with hydrogen pre-treatment.

well as the increase of methane yield by hydrogen pre-treatment of the GDE.[22] The potential of the working electrode during the electrolysis was −1.85 V vs. Ag/AgCl in the case of without hydrogen pre-treatment, whereas that with hydrogen treatment was −1.77 V. These electrode potentials hardly changed at all during the electrolysis.

Discussion

Drastic CO Reduction in the Reverse Configuration. As shown in Table 2, drastic CO reduction was observed in the electrochemical CO reduction using Pt-GDE in the case of reverse configuration, while hydrogen was only the reduction product in the normal configuration. The electrode potential of Pt-GDE at the normal configuration electrolysis was more positive by 360 mV than that of the reverse configuration, as shown in Table 2. This suggests that hydrogen is easily formed by reduction of water with a lower overpotential on a Pt catalyst at the normal configuration, even under 20 atm of CO. At the present stage of research, we cannot explain clearly the reason why high efficient CO reduction was observed only in the case of the reverse configuration of Pt-GDE. Effect of the reverse configuration might be effective for preventing the hydrogen formation due to the hydrophobicity of the gas diffusion layer, as has been described in the previous paper.[22]

In the case of electrolysis on the GDE without Pt catalyst, hydrogen was preferentially formed at more than 90% of faradaic efficiencies regardless of the configuration of the electrode, as shown in Table 2. However, methane was produced at 2.8% even without a Pt catalyst at the reverse configuration. This result suggests that CO can be also reduced to hydrocarbons and alcohols on carbon support.

Effects of the Current Density and CO Pressure. In the current density dependence of faradaic efficiencies of reduction products formed under 20 atm CO (Fig. 1), the main reduction product changed in the order of C2-compounds, methane, and hydrogen with increasing the current density. In the CO pressure dependence at 200 mA cm^{-2}, the main reduction product changed in the order of hydrogen, methane, and C2-compounds with increasing the CO pressure, as shown in Fig. 3.

The results of the current density and CO pressure dependencies of faradaic efficiencies of reduction products can be explained by the following supposition. Under the conditions of low current density and/or high pressure of CO, it is thought that CO is adsorbed sufficiently on the reaction sites of the catalyst surface because of sufficient supply of CO, resulting in prevention of adsorbed H formation. Taking into consideration the assumption that CO is reduced to hydrocarbons and alcohols by the reaction with adsorbed H, the electrocatalytic activity of the CO reduction is low under the condition of low concentration of adsorbed H on the reaction sites, so that the activity of hydrogenation of CO is low. As a result, oxygen-containing compounds such as ethanol and acetic acid, which are lower reducible products from CO, are preferentially formed as main CO reduction products under the conditions of low current density and/or high pressure of CO.

Under the conditions of large current density and/or low pressure of CO, a large number of electrons from the electrocatalyst are consumed to reduce water (protons), resulting in the formation of a high concentration of adsorbed H on the reaction site. As a result, methane, which is the highest reduction product of CO, is thought to be formed as the main CO reduction product because of the increase in the concentration of the adsorbed H. At larger current density and lower CO pressure, compared with the condition at which methane is preferentially formed, hydrogen molecules are predominantly produced by the recombination of adsorbed H because of the mass-transfer-limited supply of CO to the reaction sites. In summary, the balance between adsorbed CO and adsorbed H formed on the electrocatalyst is controlled by the balance between the current density of electrons) and the CO pressure (concentration), which determines the selectivity of the reduction products.

It was been found by UCC Co., Ltd. that acetic acid, ethanol, and acetaldehyde were produced from CO and H_2 catalyzed by Rh/SiO_2 heterogeneous catalyst at 220 °C under 210 atm.[23,24] Hydrocarbons such as methane were also produced as co-products in this reaction. It was shown that acetic acid is preferentially produced on this catalyst, at low temperature and at low partial pressure of hydrogen and high partial pressure of CO. In the electrochemical reduction of CO using a Pt-GDE, preferential formation of acetic acid was observed under the conditions of low current density and high pressure of CO, i.e. low concentration of adsorbed H and high concentration of CO in the same condition as

the reaction on Rh/SiO_2 catalyst. Taking into consideration this fact, it is suggested that the balance of concentration of adsorbed species formed on the electrocatalyst is one of the important factors in the electrochemical system that determine the selectivity of reduction product, in the same way as the heterogeneous catalytic reactions. In the case of the electrocatalytic reaction, it can be said that the product selectivity is controlled by the current density (or the electrode potential) and the supply of the reactant. In fact, we have already shown that the selectivity of the product of CO_2 reduction formed on a Cu electrode in an aqueous electrolyte depends strongly on the balance between the current density and supply of CO_2 to the electrode surface.[6,25]

Comparison between the CO_2 Reduction and CO Reduction. As shown in the electrochemical reduction of CO_2[21,22] and CO under high pressure using a Pt-GDE at the reverse configuration, methane was produced not only from CO_2, but also from CO at a high faradaic efficiency and at a large partial current density. These results suggest that CO is the first intermediate of methane formation in the electrochemical CO_2 reduction, as has been already suggested in the case of a Cu electrode in aqueous electrolytes by Hori et al.[10] Interestingly, highly efficient formation of acetic acid was observed in the electrochemical CO reduction, while no acetic acid formation was observed in the CO_2 reduction even on a Pt-GDE. This result suggests the importance of CO concentration and the reaction paths in which adsorbed CO and/or gaseous CO participate as an important reactant, such as insertion of CO into methyl group ($-CH_3$) and/or carbene ($:CH_2$) in formation of acetic acid. In the case of the electrochemical CO_2 reduction, although CO is formed by the electrochemical CO_2 reduction, concentration of CO near the electrocatalyst, is thought to be much less than that under the condition of high pressure CO. In addition, the result that CO is hardly reduced under CO 1 atm even on Pt-GDE at the reverse configuration as shown in Fig. 3, suggests that high concentration of CO is needed for the CO reduction with a high faradaic efficiency. Drastic increase in the concentration of CO must increase the reaction rate of acetic acid formation in the CO reduction, compared with the electrochemical CO_2 reduction.

Faradaic efficiencies of ethylene and ethanol formed in the CO reduction were higher than those in the CO_2 reduction. In the case of the electrochemical CO_2 reduction, for example, faradaic efficiencies of ethylene and ethanol formed on a Pt-GDE at the reverse configuration at 200 mA cm^{-2} under CO_2 30 atm were 0.6 and 1.2%, respectively[21] In the case of CO reduction, ethylene and ethanol were produced at faradaic efficiency of 9.4 and 5.1%, respectively, at 200 mA cm^{-2} under 20 atm CO. The result that faradaic efficiencies of ethylene and ethanol formations in the CO reduction are larger than those in the CO_2 reduction, suggests that CO also takes part in the formation of ethylene and ethanol and the concentration of CO is important for these reactions in the same way as the acetic acid formation.

Mechanism of Formation of HCHO and CH_4. The reaction schemes proposed from the results obtained in the present experiment are given in Fig. 8. Firstly, let us discuss formation of C1-compounds, formaldehyde and methane. Formaldehyde is thought to be formed via formyl species ($-CHO$) which was formed by the reduction of adsorbed CO (step 1). Formyl species is subsequently reduced to formaldehyde (step 3), as shown in Fig. 8. In this scheme, it is assumed that the reduction of carbon species is due reaction with adsorbed H. No methanol is formed in this electrocatalytic reaction, while formaldehyde and methane are formed as reduction products of C1-compounds.

Gladysz et al. investigated the reduction of carbonyl complex such as $[Re(C_5H_5)(CO)_2NO]$ and $[Mo(CH_3)(C_5H_5)(CO)_2(PPh_3)]$ with hydride compounds (BH_3 and $Li[BH(C_2H_5)_3]$) as a model reaction of the Fischer–Tropsch reaction.[26] They reported that formyl complex ($-CHO$) was formed by the reduction of carbonyl complex ($-CO$) and methyl complex ($-CH_3$) was formed by the reduction of formyl complex. However, no methanol or hydroxymethyl complex ($-CH_2OH$) were produced. Taking into consideration their result, it may be possible that formyl species formed by reduction of adsorbed CO is reduced to methyl species (step 4), resulting in formation of methane (step 6), so that no methanol formation was observed and only

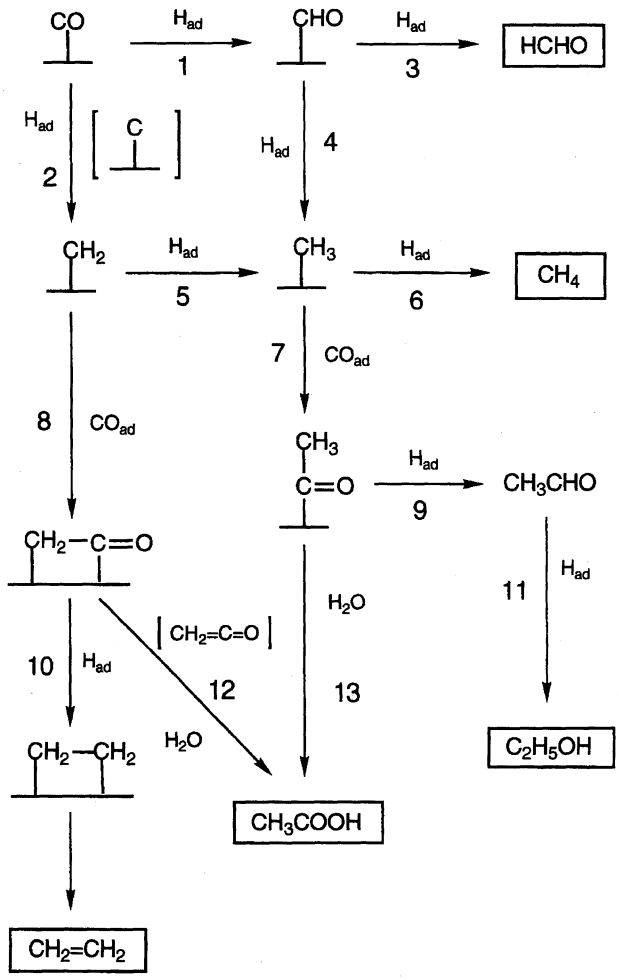

Fig. 8. Reaction schemes of the electrocatalytic Fischer–Tropsch reactions.

formaldehyde and methane were produced in the reaction on the Pt-GDE. An intermediate of methanol formation in the heterogeneous catalytic processes is thought to be methoxy species (CH_3O–). For example, Takezawa et al. supposed that Zn methoxy (CH_3O–) species was an intermediate for methanol formation from CO_2 on Cu/ZnO catalyst.[27] On the other hand, formation of methoxy species has never been observed in the electrocatalytic and electrochemical reduction of CO_2 and CO using various electrodes.

Hori et al. investigated the electrochemical reduction of aldehydes on a Cu electrode at a constant current density of 2.5 mA cm^{-2} in 0.1 mol dm^{-3} $KHCO_3$ aqueous electrolyte.[28] They reported that ethanol was formed at a faradaic efficiency of 92% form acetaldehyde. However, faradaic efficiency of methanol formation from formaldehyde was only 10%. This result indicates that it is difficult to reduce formaldehyde to methanol by the electrode reaction and formaldehyde is not the intermediate of methanol formation.

Next, let us discuss methane formation. Methane is thought to be produced by the reduction of methyl species (step 6) via formation of carbene species (: CH_2) by the reduction of adsorbed CO (step 2) and/or the reduction of formyl species (step 4). In the electrocatalytic reduction of CO on a Pt-GDE, the yield of methane was much larger than that of formaldehyde at most electrolysis conditions, as has been shown above. This result suggests that methane is produced on a Pt-GDE from CO because of the high activity of the reduction (hydrogenation), compared with formation of formaldehyde which is an intermediate reduction product. Generally, carbide (or atomic carbon) formed on the surface of the catalyst by dissociation of adsorbed CO, is assumed as an intermediate for hydrocarbon formation in the Fischer–Tropsch reaction.[29—32] Carbide is hydrogenated to carbene species (step 2) and methyl species (step 5). Frese et al. suggested that atomic carbon is the intermediate of methane formation in the electrochemical reduction of CO_2 and CO on the Ru electrode in aqueous solutions form the results of Auger electron spectroscopy analysis of the electrode surface after the electrolysis.[11,33] At the present stage of this research, however, it is not clear whether methyl species, which is thought to be an intermediate for methane formation, is formed via dissociative steps (steps 2 and 5) or non-dissociative steps (steps 1 and 4). It may be possible that the mechanism of hydrocarbon formation in the electrocatalytic of CO and CO_2 on a Pt-GDE is different form the Fischer–Tropsch reaction in the heterogeneous catalyst system.

Mechanism of Formation of C2-Compounds. Next, let us discuss the mechanism of formation of C2-compounds such as ethylene, ethanol, and acetic acid. In the Tafel plot of reduction products shown in Fig. 6, the partial current densities of methane and ethanol are constant at negative potential lower than −1.85 V vs. Ag/AgCl. This might be caused by the mass transfer limitation of CO. On the other hand, after the mass transfer limitation, the partial current densities of ethylene and acetic acid decrease with increasing the electrode potential in the cathodic direction. Temperature dependence of acetic acid also showed the same tendency as ethylene, as shown in Fig. 5. These results suggest that ethylene and acetic acid are formed by a similar reaction path and the mechanism of ethanol formation is close to the pathway of methane formation. The reaction schemes of formation of C2-compounds suggested from these results are shown in Fig. 8.

Ethanol is thought to be formed by the insertion of absorbed CO (or CO molecule) into methyl species (step 7), resulting in formation of acetyl species (CH_3CO–). Acetyl species is reduced to acetaldehyde (step 9), and ethanol is subsequently formed by reduction of acetaldehyde (step 11). Formation of acyl group (RCO–) by insertion of CO into alkyl group (e.g. step 7) has been well-known as the key step of many homogeneous catalytic reactions such as the hydroformyl reactions (Oxo reactions) and Reppe reactions. The insertion of CO into alkyl group may also take place in formation of C3-compounds such as 1-propanol and allyl alcohol.

On the other hand, ethylene and acetic acid may be formed via insertion of CO into carbene (step 8), resulting in formation of ketene (CH_2=C=O). Ketene is subsequently reduced to ethylene (step 10) or reacts with water to produce acetic acid (step 12), as shown in Fig. 8. Takeuchi et al. suggested that ketene formed by insertion of CO into carbene species (: CH_2) is the intermediate in the formation of ethanol from CO and H_2 catalyzed by Rh/TiO_2 catalyst in the Fischer–Tropsch reaction.[34] In the reaction of the present experiment using a Pt-GDE, it can be supposed that ketene formed on the reaction site reacts with water to produce acetic acid due to the presence of a large amount of water in the electrolyte. It is possible that dimerization of carbene takes place to form ethylene.

As shown in the Tafel plot (Fig. 6), the partial current densities of ethylene and acetic acid formations decrease with increasing the electrode potential in the cathodic direction. At negative potential, concentration of adsorbed H increases, leading to the increase in hydrogenation activity with adsorbed H. Under this condition, carbene is preferentially consumed in formation of methyl species (step 5), suppressing the formation of ethylene and acetic acid (step 8,10, and 12). On the other hand, methane formation by the hydrogenation of methyl species remains nearly constant because of preferential consumption of carbene to methyl species (step 5) even under the mass transfer limitation of CO. This is thought to be the reason why the partial current densities of ethylene and acetic acid decrease at negative potential and that of methane remains constant.

There are several processes of acetic acid synthesis catalyzed by metal complexes in homogeneous systems. In Monsanto process, carbonylation of methanol to acetic acid catalyzed by Rh complex at 150—200 °C under 30 atm, is well-known and conducted as an industrial synthesis process of acetic acid.[35] In this system, Rh acetyl complex (CH_3CO–Rh) produced by insertion of CO into methyl group (CH_3–Rh), is thought to be the intermediate, which is hydrolyzed to acetic acid.[36] Fujiwara et al. found that acetic acid is

produced from methane and CO[37—39] or CO_2[40] catalyzed by $Pd(OAc)_2/Cu(OAc)_2$ catalyst. Moreover, Lin et al. reported the catalytic conversion of methane into acetic acid with CO and O_2, catalyzed by $RuCl_3$ catalyst in aqueous medium at 100 °C.[41] In these catalytic reactions, it has been also proposed that acetyl that acetyl complex is the intermediate in the formation of acetic acid. Taking into consideration these reaction mechanisms of acetic acid formation, it might be possible that asetic acid is also formed in the electrochemical CO reduction on the Pt-GDE by hydrolysis of acetyl species (step 13).

Possibility of the Electrocatalytic Fischer–Tropsch Reaction Fisher–Tropsch reaction is known as the heterogeneous processes of hydrocarbons and oxygen-containing compounds formation from CO and H_2, catalyzed by 8—10 group metal catalysts such as Fe, Co, Ni, Ru, Rh, Pd, and Pt. In the present experiment, is was found for the first time that hydrocarbons and alcohols were produced at high faradaic efficiencies and at large partial current density on the electrocatalytic reduction of CO using the Pt-GDE at room temperature. Sammells et al. reported the electrochemical reduction of CO under 1 atm using the GDEs loaded with dispersed Cu, Cu–Ag, and Cu–Pb electrocatalysts in a 1 mol dm^{-3} KOH aqueous electrolyte at ambient temperature.[42] As a result, methane, ethylene, and alcohols were produced at high faradaic efficiencies and at large partial current densities on these electrocatalysts. Total faradaic efficiency for CO reduction on a Cu-GDE at a constant current density of 600 mA cm^{-2} reached 98%. The results of the present experiment and those reported by Sammells et al. that hydrocarbons and alcohols are produced from CO on electrocatalysts at ambient temperature and low CO pressure conditions show the achievement of the electrocatalytic Fischer–Tropsch reactions in the electrochemical systems. The catalytic activity proceeding these catalytic reactions under even mild conditions, compared with that in the heterocatalytic systems, might be thought to be due to the electrode potential assistance. In an electrochemical system, H_2O contained in the electrolyte can be directly used as the hydrogen source. It is for the first time acetic acid is formed from CO in the electrocatalytic system of Pt-GDE. This result indicates the possible of development of the electrocatalytic Fischer–Tropsch reaction.

This work was supported by the Grant-in-Aid for Scientific Research No. 04241106 and 416303 from the Ministry of Education, Science, Sports and Culture. One of us (KH) has been granted by Research Fellowships of the Japan Society for the Promotion of Science for Young Scientists.

References

1) Y. Hori, K. Kikuchi, and S. Suzuki, *Chem. Lett.*, **1985**, 1695.
2) Y. Hori, H. Wakebe, T. Tsukamoto, and O. Koga, *Electrochim. Acta*, **39**, 1833 (1994).
3) S. Ikeda, T. Takagi, and K. Ito, *Bull. Chem. Soc. Jpn.*, **60**, 2517 (1987).
4) H. Noda, S. Ikeda, Y. Oda, K. Imai, M. Maeda, and K. Ito, *Bull. Chem. Soc. Jpn.*, **63**, 2459 (1990).
5) M. Azuma, K. Hashimoto, M. Hiramoto, M. Watanabe, and T. Sakata, *J. Electrochem. Soc.*, **137**, 1772 (1990).
6) K. Hara, A. Tsuneto, A. Kudo, and T. Sakata, *Shokubai (Catalyst)*, **35**, 513 (1993).
7) K. Hara, A. Kudo, and T. Sakata, *J. Electroanal. Chem.*, **391**, 141 (1995).
8) Y. Hori, K. Kikuchi, A. Murata, and S. Suzuki, *Chem. Lett.*, **1986**, 897.
9) Y. Hori, A. Murata, R. Takahashi, and S. Suzuki, *J. Chem. Soc., Chem. Commun.*, **1988**, 17.
10) Y. Hori, A. Murata, and R. Takahashi, *J. Chem. Soc., Faraday Trans. 1*, **85**, 2309 (1989).
11) D. P. Summers and K. W. Frese, Jr., *Langmuir*, **4**, 51 (1988).
12) Y. Hori and A. Murata, *Electrochim. Acta*, **35**, 1777 (1990).
13) M. Azuma, K. Hashimoto, M. Watanabe, and T. Sakata, *J. Electroanal. Chem.*, **294**, 299 (1990).
14) S. Nakagawa, A. Kudo, M. Azuma, and T. Sakata, *J. Electroanal. Chem.*, **308**, 339 (1991).
15) A. Kudo, S. Nakagawa, A. Tsuneto, and T. Sakata, *J. Electrochem. Soc.*, **140**, 1541 (1993).
16) K. Hara, A. Kudo, and T. Sakata, *J. Electroanal. Chem.*, **386**, 257 (1995).
17) R. L. Cook, R. C. MacDuff, and A. F. Sammells, "Proceeding of International Symposium on Chemical Fixation of Carbon Dioxide," Nagoya (1991), p. 39.
18) A. F. Sammells and R. L. Cook, in "Electrochemical and Electrocatalytic Reactions of Carbon Dioxide," ed by B. P. Sullivan, K. Krist, and H. E. Guard, Elsevier Sci. Pub., Amsterdam (1993), p. 255.
19) Y. Hori, O. Koga, A. Aramata, and M. Enyo, *Bull. Chem. Soc. Jpn.*, **65**, 3008 (1992).
20) Y. Hori, A. Murata, T. Tsukamoto, H. Wakebe, O. Koga, and H. Yamazaki, *Electrochim. Acta*, **39**, 2495 (1994).
21) K. Hara, A. Kudo, T. Sakata, and M. Watanabe, *J. Electrochem. Soc.*, **142**, L57 (1995).
22) K. Hara and T. Sakata, *J. Electrochem. Soc.*, In press.
23) Japan Patent 80806 by UCC, (1976).
24) Japan Patent 41568 by UCC, (1979).
25) K. Hara, A. Tsuneto, A. Kudo, and T. Sakata, *J. Electrochem. Soc.*, **141**, 2097 (1994).
26) W. Tam, W. Wong, and J. A. Gladysz, *J. Am. Chem. Soc.*, **101**, 1589 (1979).
27) S. Fujita, M. Usui, E. Ohara, and N. Takezawa, *Catal. Lett.*, **13**, 349 (1992).
28) Y. Hori, Y. Ide, N. Yokoyama, A. Murata, and O. Koga, "Proceeding of Symposium on Fixation of Carbon Dioxide," Nagoya (1992), p. 49.
29) F. Fischer and H. Tropsch, *Brennst. Chem.*, **7**, 97 (1926).
30) P. R. Wentrcek, B. J. Wood, and H. Wise, *J. Catal.*, **43**, 363 (1976).
31) M. Araki and V. Ponec, *J. Catal.*, **44**, 439 (1976).
32) R. C. Brady, III, and R. Pettit, *J. Am. Chem. Soc.*, **103**, 1287 (1981).
33) D. P. Summers and K. W. Frese, Jr., *J. Electrochem. Soc.*, **135**, 264 (1988).
34) A. Takeuchi and J. R. Katzer, *J. Phys. Chem.*, **86**, 2438 (1982).
35) F. E. Paulik and J. F. Roth, *J. Chem. Soc., Chem. Commun.*, **1968**, 1578.
36) D. Forster, *Adv. Organomet. Chem.*, **17**, 255 (1979).

37) T. Nishiguchi, K. Nakata, K. Takaki, and Y. Fujiwara, *Chem. Lett.*, **1992**, 1141.
38) K. Nakata, T. Miyata, T. Jintoku, A. Kitani, Y. Taniguchi, K. Takaki, and Y. Fujiwara, *Bull. Chem. Soc. Jpn.*, **66**, 3755 (1993).
39) K. Nakata, Y. Yamaoka, T. Miyata, Y. Taniguchi, K. Takaki, and Y. Fujiwara, *J. Organomet. Chem.*, **473**, 329 (1994).
40) M. Kurioka, K. Nakata, T. Jintoku, Y. Taniguchi, K. Takaki, and Y. Fujiwara, *Chem. Lett.*, **1995**, 244.
41) M. Lin and A. Sen, *Nature*, **368**,613 (1994).
42) M. Schwartz, M. E. Vercauteren, and A. F. Sammells, *J. Electrochem. Soc.*, **141**, 3119 (1994).